

# The VISTA Near-infrared YJKs Public Survey of the Magellanic Clouds System (VMC)

Maria-Rosa Cioni<sup>1, 2</sup>  
 Gisella Clementini<sup>3</sup>  
 Leo Girardi<sup>4</sup>  
 Roald Guandalini<sup>1</sup>  
 Marco Gullieuszik<sup>5</sup>  
 Brent Miszalski<sup>1</sup>  
 Maria-Ida Moretti<sup>6</sup>  
 Vincenzo Ripepi<sup>7</sup>  
 Stefano Rubele<sup>4</sup>  
 Gemma Bagheri<sup>1</sup>  
 Kenji Bekki<sup>8</sup>  
 Nick Cross<sup>9</sup>  
 Erwin de Blok<sup>10</sup>  
 Richard de Grijs<sup>11</sup>  
 Jim Emerson<sup>12</sup>  
 Chris Evans<sup>13</sup>  
 Brad Gibson<sup>14</sup>  
 Eduardo Gonzales-Solares<sup>15</sup>  
 Martin Groenewegen<sup>5</sup>  
 Mike Irwin<sup>15</sup>  
 Valentin Ivanov<sup>16</sup>  
 Jim Lewis<sup>15</sup>  
 Marcella Marconi<sup>7</sup>  
 Jean-Baptiste Marquette<sup>17, 18</sup>  
 Chiara Mastrogiuseppe<sup>19</sup>  
 Ben Moore<sup>20</sup>  
 Ralf Napiwotzki<sup>1</sup>  
 Tim Naylor<sup>21</sup>  
 Joana Oliveira<sup>22</sup>  
 Mike Read<sup>9</sup>  
 Eckhard Sutorius<sup>9</sup>  
 Jacco van Loon<sup>22</sup>  
 Mark Wilkinson<sup>23</sup>  
 Peter Wood<sup>24</sup>

- <sup>1</sup> University of Hertfordshire, Physics Astronomy and Mathematics, United Kingdom
- <sup>2</sup> University Observatory Munich, Germany
- <sup>3</sup> INAF, Osservatorio Astronomico di Bologna, Italy
- <sup>4</sup> INAF, Osservatorio Astronomico di Padova, Italy
- <sup>5</sup> Royal Observatory of Belgium, Belgium
- <sup>6</sup> University of Bologna, Department of Astronomy, Italy
- <sup>7</sup> INAF, Osservatorio Astronomico di Capodimonte, Italy
- <sup>8</sup> ICRAR, University of Western Australia, Australia
- <sup>9</sup> University of Edinburgh, Institute for Astronomy, United Kingdom
- <sup>10</sup> University of Cape Town, South Africa
- <sup>11</sup> Peking University, Kavli Institute for Astronomy and Astrophysics, China
- <sup>12</sup> Queen Mary, University of London, United Kingdom

- <sup>13</sup> UK Astronomy Technology Centre, United Kingdom
- <sup>14</sup> Centre for Astrophysics, University of Central Lancashire, United Kingdom
- <sup>15</sup> University of Cambridge, Institute of Astronomy, United Kingdom
- <sup>16</sup> ESO
- <sup>17</sup> UPMC, University of Paris, Institut d'Astrophysique de Paris, France
- <sup>18</sup> CNRS, Institut d'Astrophysique de Paris, France
- <sup>19</sup> LERMA, Observatoire de Paris, France
- <sup>20</sup> University of Zurich, Institute of Theoretical Physics, Switzerland
- <sup>21</sup> University of Exeter, School of Physics, United Kingdom
- <sup>22</sup> University of Keele, School of Physical and Geographical Sciences, United Kingdom
- <sup>23</sup> University of Leicester, United Kingdom
- <sup>24</sup> Mount Stromlo Observatory, RSSA, Australia

The VISTA public survey project VMC targets the Large Magellanic Cloud, the Small Magellanic Cloud, the Bridge and two fields in the Stream. The VMC survey is a uniform and homogeneous survey in the Y, J and K<sub>s</sub> near-infrared filters. The main goals are the determination of the star formation history and the three-dimensional structure of the Magellanic system. The survey is therefore designed to reach stars as faint as the oldest main sequence turn-off point and to constrain the mean magnitude of pulsating variable stars such as RR Lyrae and Cepheids. We provide a brief overview of the survey strategy and first science results. Further details are given in Cioni et al. (2011).

## Introduction

The Magellanic Clouds offer an excellent laboratory for near-field cosmology. They represent the closest prototype for studies of interacting galaxies and their low metallicity and high gas content provide information about galaxies at an early stage of evolution. The Magellanic Clouds have experienced an extended star formation history (SFH) and their dynamical interaction may be responsible for the formation of the Magellanic Bridge. The origin of the Magellanic Stream is under

debate as to whether it is also of tidal origin from the interaction of the Large Magellanic Cloud (LMC) with the Small Magellanic Cloud (SMC), or produced by ram pressure between the two galaxies.

The VMC<sup>1</sup> survey is acquiring near-infrared (NIR) data of unprecedented sensitivity in the Magellanic system that is of immense value for the astronomical community. The survey represents the only NIR counterpart to existing optical surveys and for the large number of unclassified objects observed with the Spitzer Space Telescope in the mid-infrared. The VMC will cover the bulk of the Magellanic system as opposed to the tiny regions sampled by the Hubble Space Telescope, and the limited area covered by most of the other ground-based observations at the same sensitivity.



Figure 1. VMC logo

Current open questions about the formation and evolution of the Magellanic Clouds will be addressed by the VMC survey, such as: How have the SFHs of the LMC and SMC been influenced by interaction? Does the geometry of the Magellanic system depend on age and metallicity? Why is there a significant difference in structure between the gas and stars in the SMC?

## Observations and data reduction

VISTA<sup>2</sup> (Emerson et al. 2006) is the largest wide-field NIR imaging telescope designed to perform survey operations. The performance during commissioning is presented by Emerson et al. (2010), while science verification programmes are summarised in Arnaboldi et al. (2010).

The VMC survey parameters are listed in Table 1. VMC uses three filters,  $Y$ ,  $J$  and  $K_s$  for the analysis of colour–colour diagrams; the wider colour spacing in  $Y$ – $K_s$  provides a good characterisation of the sub-giant branch population for deriving the SFH. Monitoring of variable sources is performed in the  $K_s$ -band, where variable stars obey a clear period–magnitude relation. The VMC survey area is shown in Figure 2. It covers the area to a limiting  $B$  magnitude of 25 mag arc-sec<sup>-2</sup> for both galaxies and encompasses the major features traced by the distribution of stars and gas.

Here we focus on observations obtained during the dry-run period (November 2009–March 2010) when VISTA was tested and survey operations were still being defined. Six VMC fields were

observed in the LMC. One field covers the famous 30 Doradus region, one field corresponds to the South Ecliptic Pole (SEP) region, there are a pair of fields located in the northern outer part of the LMC disc while the remaining two fields are located towards the Bridge. The progress of the VMC survey observations up to 4 March 2011 is provided in Table 2.

The VISTA raw images are reduced by the VISTA Data Flow System (VDFS) pipeline at the Cambridge Astronomical Survey Unit (CASU<sup>3</sup>). Standard reduction steps are performed and quality control parameters are calculated for both monitoring and evaluating observing conditions retrospectively. A tile image is produced by combining different pawprint images adjusted for astrometric and photometric distortions as well as different

sky levels. Tile catalogues are produced following the application of a nebulousity filter in order to remove diffuse varying background on scales of 3 arcseconds or larger (Irwin 2010). The average VMC parameters from all single-tile images are given in Table 3 where the magnitude limit is at  $5\sigma$ . This set comprises observations obtained up to the end of November 2010 but does not distinguish between crowded and uncrowded fields for which the VMC has different observing requirements.

Astrometry is based on the positions of the many 2MASS sources within each detector. The median astrometric root-mean-square is 80 milliarcseconds (mas) and is dominated by uncertainties on 2MASS coordinates. Residual systematic distortions across the VISTA field of view are present at the 25 mas level. The photometric calibration relies on the observation of stars from the 2MASS catalogue with magnitudes in the range 12–14 in all bands. The calibration in the  $Y$ -band is possible where the extinction is not too high, i.e.  $E_{B-V} < 1.5$  (Hodgkin et al. 2009). Figure 3 shows the behaviour of VISTA photometric uncertainties in a VMC field. Uncertainties are reduced by about 50% compared to those for individual tiles and will reduce further for deep tiles. A morphological classification flag is also included in the catalogue.

The data reduced by the VDFS pipeline are ingested into the VISTA Science Archive<sup>4</sup> (VSA). At present these data are reduced with the version 1.0 of the pipeline and include all VMC data observed until end of November 2011. At the VSA the data are archived to produce standardised data products: individual passband frame association and source association to provide multi-colour, multi-epoch source lists; cross-associations with external catalogues; and deeper stacking. The position and magnitude of each source in a given table refers to the astrometrically and photometrically calibrated measurements using the parameters specified in the image headers. In addition the magnitude of the brightest stars ( $K_s < 12$  mag.) are recovered for saturation effects (Irwin 2009). Figure 4 shows the  $K_s$  magnitude difference for stars in a VMC field compared to 2MASS before and after saturation correction.

Table 1. VMC survey parameters.

Filter	$Y$	$J$	$K_s$	Filter	$Y$	$J$	$K_s$
Central $\lambda$ ( $\mu\text{m}$ )	1.02	1.25	2.15	Exposure time per epoch (s)	800	800	750
Bandwidth ( $\mu\text{m}$ )	0.10	0.18	0.30	No. of epochs	3	3	12
DIT (s)	20	10	5	Total exposure time (s)	2400	2400	9000
No. of DITs	4	8	15	Sensitivity per epoch (Vega)	21.3	20.8	18.9
No. of exposures	1	1	1	S/N per epoch	5.7	5.9	2.9
Micro-stepping	1	1	1	Total sensitivity (Vega)	21.9	21.4	20.3
No. of jitters	5	5	5	Total S/N	10	10	10
Pawprints in tile	6	6	6	Saturation (Vega)	12.9	12.7	11.4
Pixel size (arcsec)	0.339	0.339	0.339	Area (deg <sup>2</sup> )	184	184	184
System FWHM	0.51	0.51	0.51	No. of tiles	110	110	110

Description	VMC	LMC	SMC	Bridge	Stream
No. of tiles	110	68	27	13	2
No. of epochs	1980	1224	486	234	36
No. of $Y$ epochs	330	204	81	39	6
No. of $J$ epochs	330	204	81	39	6
No. of $K_s$ epochs	1320	816	324	156	24
Observed $Y$ epochs	59	37	8	8	6
Observed $J$ epochs	58.5	38.5	6.5	7.5	6
Observed $K_s$ epochs	98.5	75	5	4.5	14
No. of observed epochs	216	150.5	19.5	20	26
Completion in $Y$	17.9%	18.1%	9.9%	20.5%	100%
Completion in $J$	17.7%	18.9%	8%	19.2%	100%
Completion in $K_s$	7.5%	9.2%	1.5%	2.9%	58.3%
<b>Total completion</b>	<b>10.9%</b>	<b>12.3%</b>	<b>4%</b>	<b>8.5%</b>	<b>72.2%</b>

Table 2. VMC survey progress up to 4 March 2011. (Items in blue refer to the complete survey.)

Filter	FWHM	Ellipticity	Zero-point	Mag. Limit
$Y$	1.03 (0.14)	0.06 (0.01)	23.44 (0.10)	21.00 (0.49)
$J$	1.01 (0.13)	0.06 (0.01)	23.68 (0.14)	20.55 (0.44)
$K_s$	0.92 (0.10)	0.05 (0.01)	23.00 (0.19)	19.25 (0.30)

Table 3. VMC survey tile quality up to 30 November 2010.

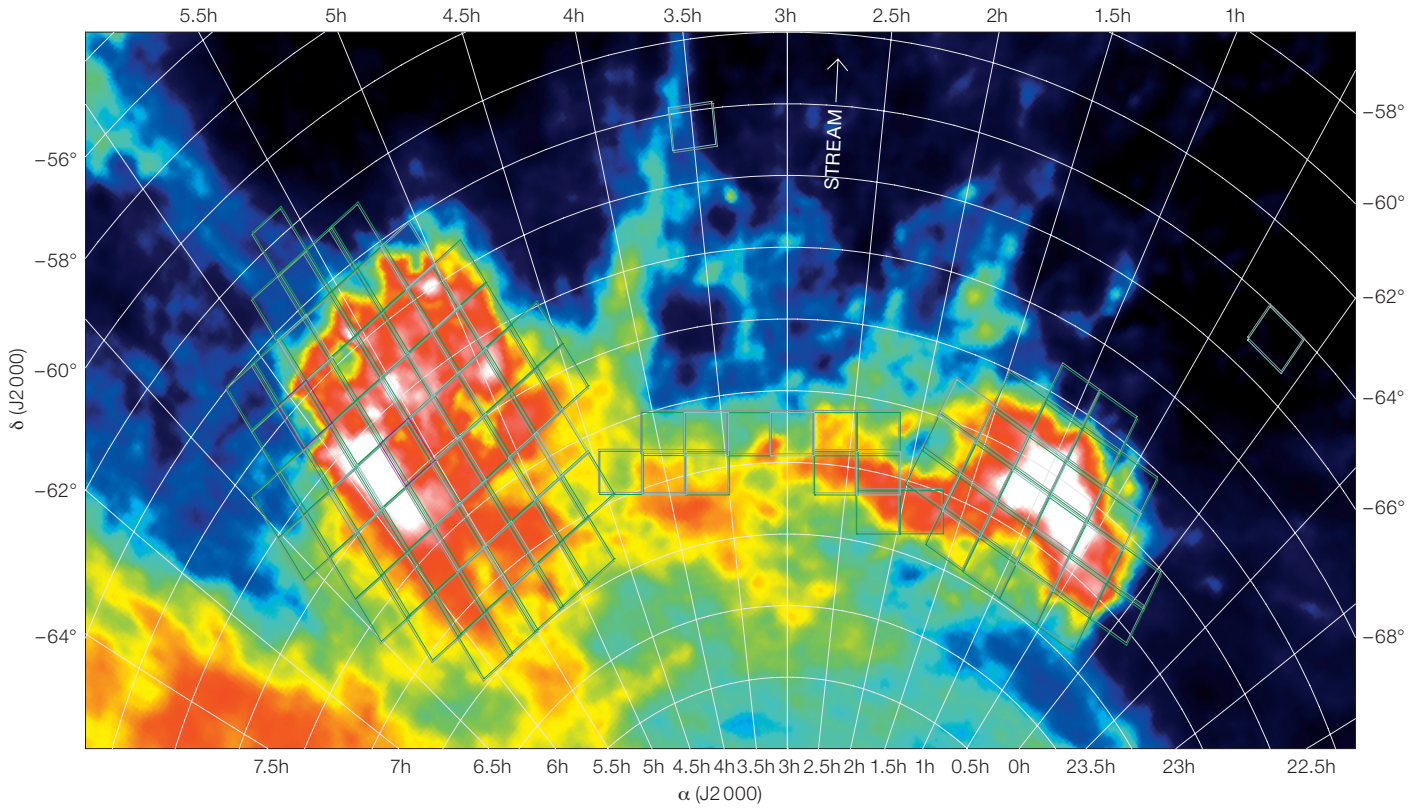
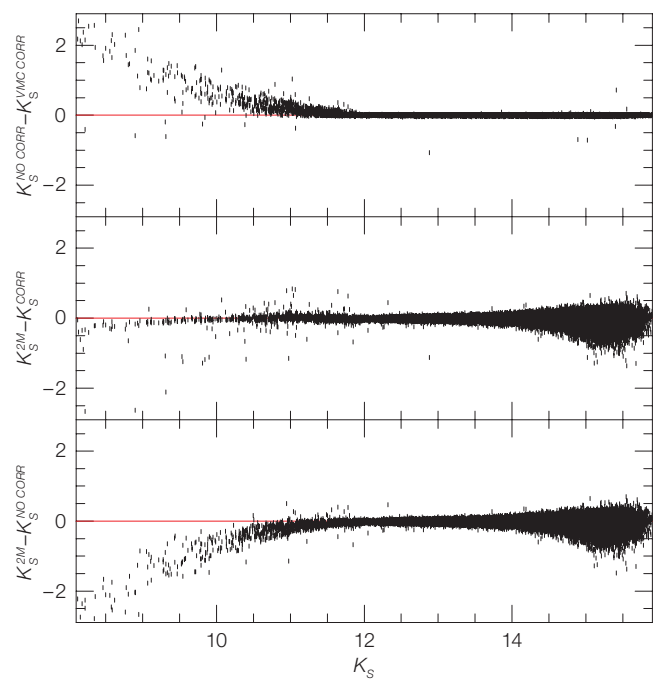
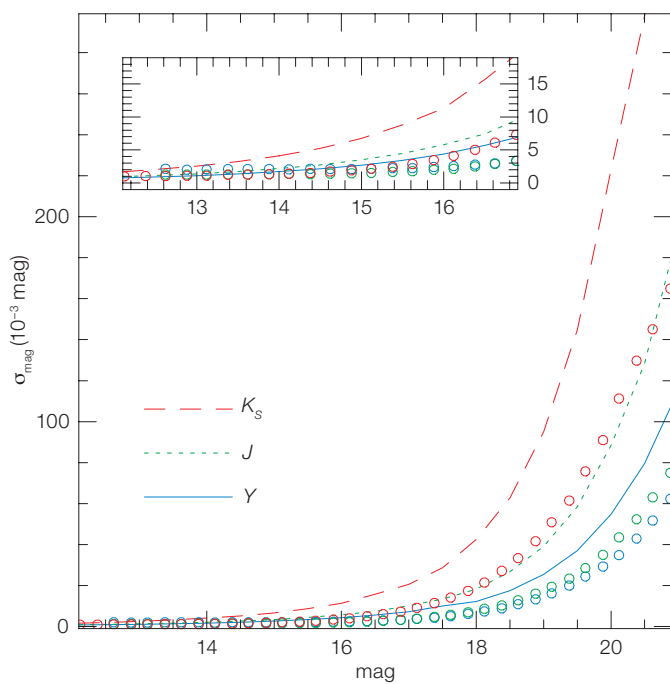


Figure 2. (Top) Magellanic system area tiled for VMC observations superimposed on the distribution of H I gas (McClure-Griffiths et al. 2009). Tiles are colour coded as follows: purple: completed; cyan: observations in progress; green: to be observed.

Figure 3. (Bottom left) Photometric uncertainties in the VMC data for stacked pawprints (dashed, dotted and continuous lines in the  $K_s$ -,  $J$ - and  $Y$ -bands respectively) and tiles (red, green and blue circles in the  $K_s$ -,  $J$ - and  $Y$ -bands respectively) in one field are shown.

Figure 4. (Bottom right) Magnitude difference for stars in common between VMC and 2MASS before (bottom) and after (middle) recovering the magnitude of VMC stars approaching the saturation limit; the adjustment applied is shown at top.



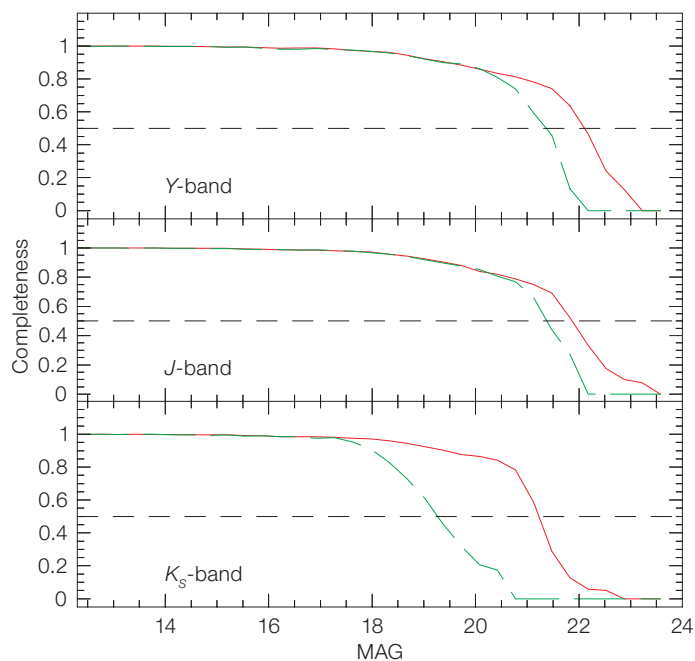


Figure 5. Completeness results for the South Ecliptic Pole (SEP) field are shown for single epoch (in green) and deep stacked images (in red).

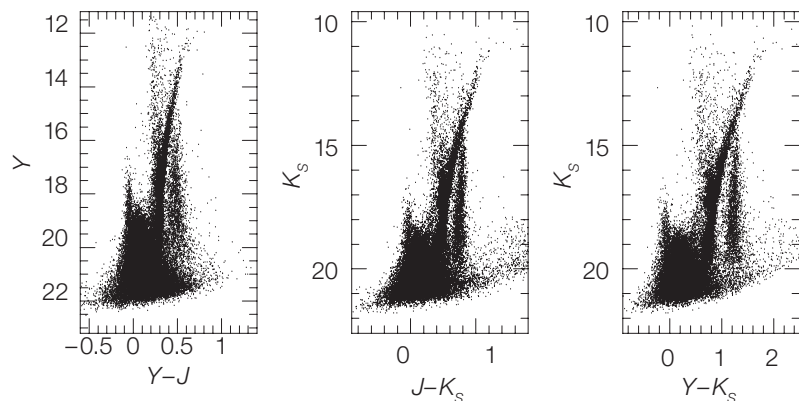


Figure 6. Colour-magnitude diagrams of VMC sources in the SEP field.

The completeness of the stellar photometry as a function of location across the Magellanic system and position in the colour-magnitude diagrams is estimated via the usual procedure of adding artificial stars of known magnitudes and positions to the images, then comparing them in the derived photometric catalogues. For this work tile images are created and regions equivalent to 1/12 of the area are selected for performing PSF photometry. Then, artificial stars are added randomly at a mutual distance of  $> 30$  pixels, so as not to increase the typical crowding of the images. Artificial stars spanning smaller bins are later grouped together to estimate the number ratio between

added and recovered stars. The results of this process are shown in Figure 5.

#### Colour-magnitude diagrams

Figure 6 shows the colour-magnitude diagrams (CMDs) of VMC stellar and probable stellar sources in the SEP field. These data were extracted from the VSA. The exposure times per band correspond to 2400 s in Y, 2800 s in J and 9400 s in  $K_s$ .

The distribution of stars in the CMDs shows different stellar populations. The bluest conic structure, bending to red colours at bright magnitudes, is formed by main sequence (MS) stars of increasing mass with increasing brightness. The MS joins, via the sub-giant branch,

the red giant branch (RGB) beginning at  $\sim 2$  mag below the red clump, the approximately circular region described by the highest concentration of stars. The RGB continues beyond the red clump at brighter magnitudes describing a narrow structure bending to red colours. The abrupt change in source density at the tip of the RGB marks the transition to brighter asymptotic giant branch (AGB) stars. The broad vertical distribution of stars below the RGB is populated by Milky Way (MW) stars that are easily distinguished from LMC stars. Cepheid and supergiant stars occupy the region of the diagram to the bright and blue side of the RGB, while RR Lyrae stars are somewhat fainter than the red clump and lie more or less parallel to the sub-giant branch.

#### The Ant diagram

Figure 7 shows the observed colour-colour diagram, and the corresponding CMDs, of the VMC data in the SEP field. The distribution of sources in the colour-colour diagram resembles the body of an ant, with different parts distinguished:

- *Gaster* ( $-0.1 < (Y-J) < 0.3$  and  $-0.3 < (J-K_s) < 0.3$ ), shown in red, the lower part of the ant body corresponds to the location of MS stars in the LMC, with the youngest being at the bluest extremity.
- *Mesosoma* ( $0.2 < (Y-J) < 0.4$  and  $0.4 < (J-K_s) < 0.75$ ), shown in blue, the middle part of the ant body corresponds to the main locus of helium-burning giants in the LMC. Most of them are in the red clump.
- *Petiole* ( $0.15 < (Y-J) < 0.3$  and  $0.3 < (J-K_s) < 0.4$ ), shown in green, is a small thin extension of the mesosoma at its red side, and is mainly caused by foreground bright stars in the MW
- *Head* ( $0.4 < (Y-J) < 0.55$  and  $0.65 < (J-K_s) < 0.85$ ), shown in magenta. Its main blob is defined by foreground low-mass stars in the Milky Way.
- *Upper antenna* ( $0.42 < (Y-J) < 0.6$  and  $0.85 < (J-K_s) < 1.1$ ), shown in cyan, being formed by the more luminous RGB stars in the LMC close to the tip of the RGB, extending up to  $(J-K_s) = 1$  mag.
- *Lower antenna* ( $(Y-J) > 0.55$  and  $0.6 < (J-K_s) < 0.85$ ), shown in yellow, corresponding to the  $(Y-J)$  redward

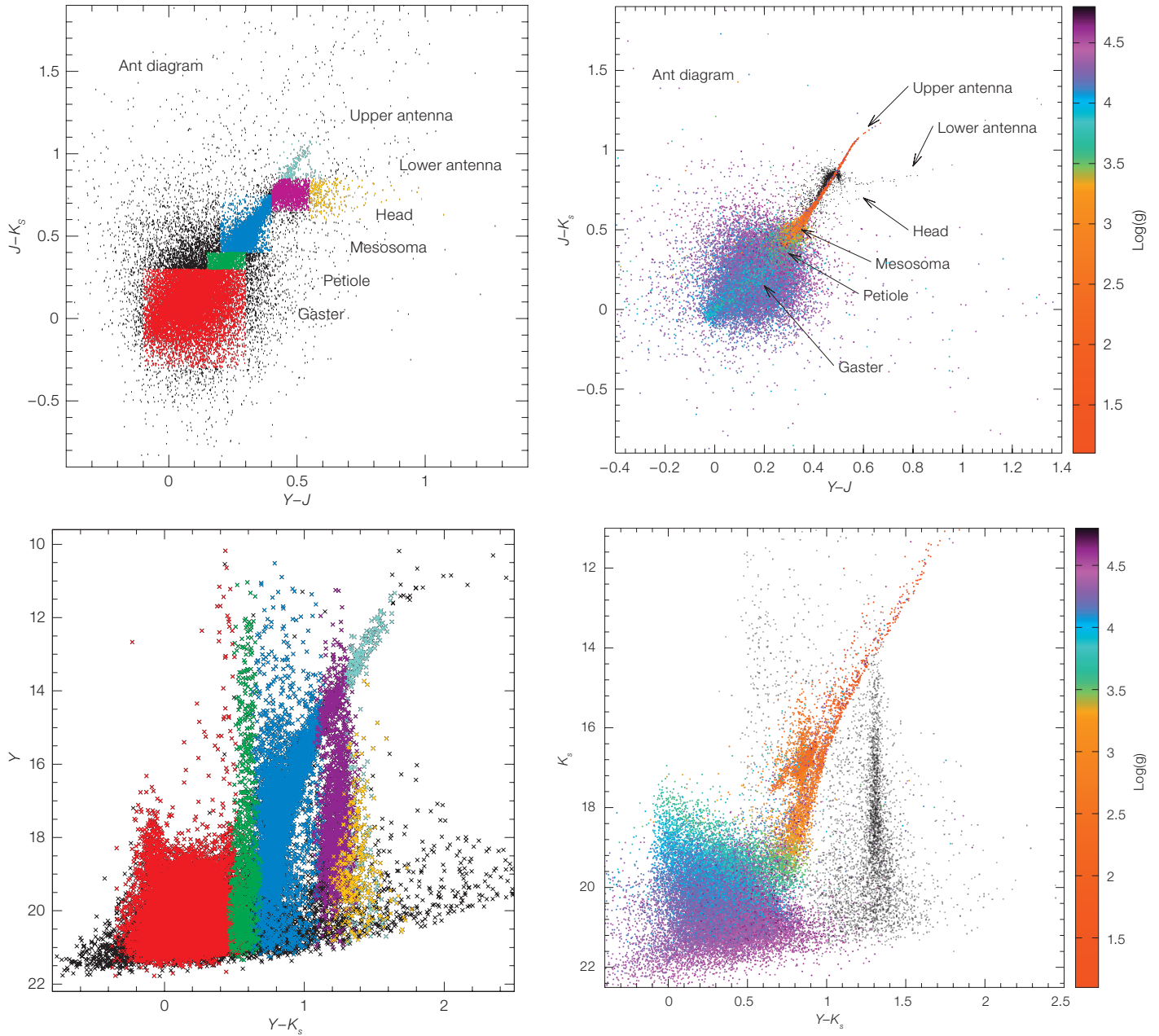


Figure 7. Colour–colour (“Ant diagrams”) and colour–magnitude (CM) diagrams of VMC sources in the SEP field are shown for observed magnitudes (upper and lower left) and simulated magnitudes (upper and lower right). In the observed magnitude plots (left column), the coloured points correspond to the morphological selection outlined in the text and labelled in the upper plot. The mapping of stellar surface gravity to the simulated colour–colour and CM diagrams is shown in the right column.

The simulated Ant diagram is also shown in Figure 7, where colours now represent the stellar surface gravity.

### RR Lyrae stars and Cepheids

Radially pulsating stars obey a period–mean density relation that forms the basis of their use as standard candles to measure the distance to the host system. In particular, RR Lyrae stars obey a period–luminosity–metallicity relation in

the  $K_s$ -band that is only weakly affected by evolutionary effects, the spread in stellar mass within the instability strip and uncertainties in reddening corrections. Similarly, the Cepheid period–luminosity relation in the  $K$ -band is much narrower than the corresponding optical relations, and less affected by systematic uncertainties in reddening and metal content.

In the context of the VMC survey, the  $K_s$  photometry is taken in time series mode in order to obtain mean  $K_s$  magnitudes

extension of foreground low-mass stars in the MW.

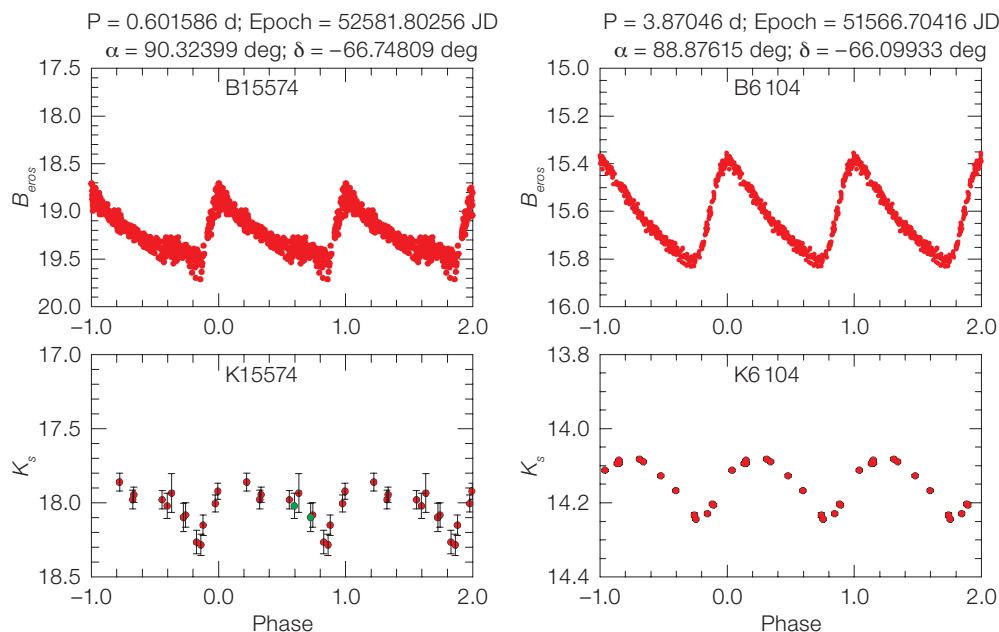


Figure 8.  $B_{EROS}$  and  $K_s$  VMC light-curves for an RR Lyrae star (left) and a Cepheid (right) in the SEP field.

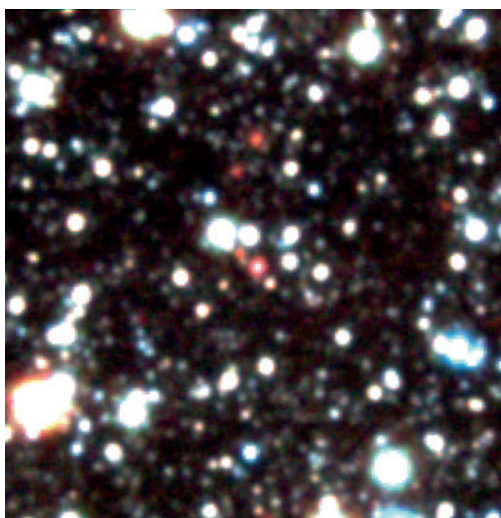
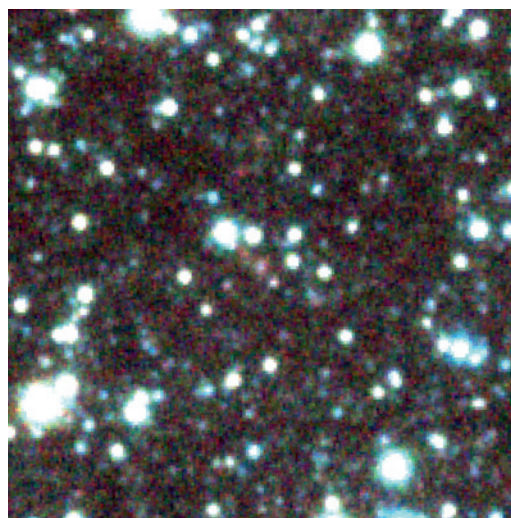


Figure 9. Colour-composite image of LMC PN MG 60 made from single (left) and stacked (right) exposures in Y (blue), J (green) and  $K_s$  (red) pass-bands.

for RR Lyrae stars and Cepheids over the whole Magellanic system. Their period–luminosity relations will be used to measure distances and construct a 3D map of the stellar distribution. The identification, period and epoch of maximum light for these objects are taken from microlensing surveys (EROS, MACHO and OGLE) of the LMC and SMC while in the Bridge we plan to use the VST data themselves (Cappellaro, 2005).

The location of the SEP field at the periphery of the LMC overlaps with EROS-2 (Tisserand et al., 2007). There

are 117 RR Lyrae and 21 Cepheids in common between EROS-2 and VMC. EROS-2 periodicities were confirmed by analysing their  $B_{EROS}$  light-curves with GRATIS (Clementini et al. 2000). Figure 8 shows  $B_{EROS}$  and VMC light-curves of the RR Lyrae star #15574 ( $P = 0.601586$  days) and the Cepheid variable #6104 ( $P = 3.87046$  days). For the RR Lyrae star there is one point per night and the magnitude is the weighted average of all available observations, while for the Cepheid two points, corresponding each to a different detector, are shown. Both light-curves are well sampled, including

shallower observations (shown in green), confirming the soundness of our observing strategy, and allowing us to derive mean magnitudes without using template light-curves. The average of individual  $K_s$  measures corresponds to  $18.02 \pm 0.12$  mag. and  $14.17 \pm 0.06$  mag. for the RR Lyrae star and Cepheid, respectively.

#### Planetary nebulae

Planetary Nebulae (PNe) are well known for their role in the development of the extragalactic standard candle planetary

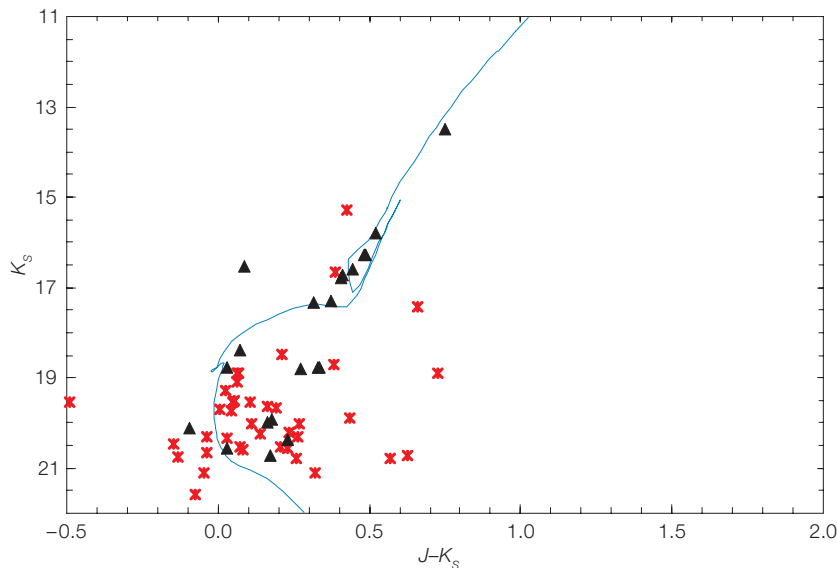


Figure 10. Colour-composite image (2 by 2 arcminutes, shown right) and CMD (shown left) of the stellar cluster KMHK 1577. The isochrone corresponds to an age of 0.63 Gyr and a metallicity of  $Z = 0.004$ .

nebula luminosity function (PNLF). Distances can be measured from the near-universal bright end cut-off across all galaxy types, but it remains difficult to explain how old stellar populations that lack recent star formation episodes could produce progenitors massive enough to power the high star luminosities populating the bright end.

Magellanic Cloud PNe are well positioned to further advance our understanding of the PNLf. The deep NIR photometry provided by the VMC survey will allow new PNe to be detected and the enhanced sensitivity to dust resulting from observation in the NIR will enable identification of contaminating compact H II regions and symbiotic stars. The synoptic nature of the VMC survey, which allows variability to be measured, will enable identification of pulsating Mira stars in the most obscured symbiotic stars, thus supporting the cleaning of the PNe sample.

Within the first six VMC tiles in the LMC, a combination of optical imaging, OGLE light-curves, the VMC NIR data and SAGE mid-infrared observations, reveals that only ~50% of the objects previously catalogued as PNe appear to be genuine. These are characterised by the colours  $0.4 < (J-K_s) < 2$  and  $0.0 < (Y-J) < 0.5$ . The non-PNe identified in the sample are

mainly misclassified field stars, compact H II regions or long-period variables. The strongest emission lines in the NIR for PNe include: H I at  $1.083 \mu\text{m}$  in Y-band, Pa  $\beta$  in J, while  $K_s$  contains Br  $\gamma$ , multiple H I and molecular H<sub>2</sub> lines. Figure 9 shows the impact of stacking individual VMC exposures to detect PNe.

### Stellar clusters

Stellar clusters are among the primary targets of the VMC survey. The detection of known stellar clusters will be examined and new clusters will be searched for. The analysis of stellar clusters will be centred on CMDs to estimate their ages and metallicities as well as on the comparison with results obtained from optical surveys. Ages, masses and metallicities of stellar clusters will allow us to discuss the SFH of the Magellanic Clouds and radial abundance gradients.

Here we show results obtained for cluster KMHK 1577 (Kontizas et al. 1990) in the SEP field. The properties of this cluster are unknown and it was chosen because of its favourable location at the centre of a pawprint. The image and CMD of the cluster are shown in Figure 10. The exposure time was 2400 s in Y, 2800 s in J

and 9400 s in  $K_s$ ; triangles indicate stellar sources and asterisks extended objects.

### Acknowledgements

The VMC survey is supported by ESO and the UK STFC. This research has made use of Aladin, EROS-2 and 2MASS data. The UK's VISTA Data Flow System comprising the VISTA pipeline at CASU and the VISTA Science Archive at the Wide Field Astronomy Unit (WFAU) in Edinburgh has been crucial in providing us with calibrated data products for this paper.

### References

- Arnaboldi, M. et al. 2010, *The Messenger*, 134, 42
- Cappellaro, E. 2005, *The Messenger*, 120, 13
- Cioni, M.-R. L. et al. 2011, *A&A*, 527, A116
- Clementini, G. et al. 2000, *AJ*, 120, 2054
- Emerson, J. et al. 2006, *The Messenger*, 126, 41
- Emerson, J. et al. 2010, *The Messenger*, 139, 2
- Hodgkin, S. T. et al. 2009, *MNRAS*, 394, 675
- Irwin, M. 2009, *UKIRT Newsletter*, 25, 15
- Irwin, M. 2010, *UKIRT Newsletter*, 26, 14
- Kontizas, M. et al. 1990, *A&A*, 84, 527
- McClure-Griffiths, N. et al. 2009, *ApJS*, 181, 398
- Tisserand, P. et al. 2007, *A&A*, 469, 387

### Links

- <sup>1</sup> VMC survey: <http://star.herts.ac.uk/~mcioni/vmc/>
- <sup>2</sup> VISual and Infrared Telescope for Astronomy (VISTA): <http://www.vista.ac.uk>
- <sup>3</sup> CASU: <http://casu.ast.cam.ac.uk/surveys-projects/vista>
- <sup>4</sup> VISTA Science Archive (VSA): <http://horus.roe.ac.uk/vsa/login.html>